

Shot noise in the self-dual Interacting Resonant Level Model

A. Branschädel

Institut für Theorie der Kondensierten Materie, Karlsruhe Institute of Technology, 76021 Karlsruhe, Germany

E. Boulat

Laboratoire MPQ, CNRS UMR 7162, Université Paris Diderot, 75205 Paris Cedex 13

H. Saleur

*Institut de Physique Théorique, CEA, IPhT and CNRS, URA2306, Gif Sur Yvette, F-91191 and
Department of Physics, University of Southern California, Los Angeles, CA 90089-0484*

P. Schmitteckert

Institute of Nanotechnology, Karlsruhe Institute of Technology, 76344 Eggenstein-Leopoldshafen, Germany

By using two independent and complementary approaches, we compute exactly the shot noise in an out-of-equilibrium interacting impurity model, the Interacting Resonant Level model at its self-dual point. An analytical approach based on the Thermodynamical Bethe Ansatz allows to obtain the density matrix in the presence of a bias voltage, which in turn allows for the computation of any observable. A time-dependent Density Matrix Renormalization Group technique, that has proven to yield the correct result for a free model (the Resonant Level Model) is shown to be in perfect agreement with the former method.

The study of transport in out of equilibrium, strongly interacting systems, is of crucial importance for technological applications. It also addresses some of the most challenging fundamental questions, from the possibility of fluctuations theorems out of equilibrium [1], to the time evolution of quantum many body entanglement [2].

While experimental progress in this area has been swift and steady (see e.g. [3–7]), the theory has been held back by considerable technical difficulties. The physics of interest occurs usually in non perturbative regimes, where analytical methods are few and limited. Numerical approaches require real time simulations, which up to recently had been notoriously difficult.

Yet the situation is changing, especially in the case of quantum impurity problems. Extensions of the Bethe ansatz to study transport properties have been proposed [8, 9], while time dependent DMRG (td-DMRG) calculations have become quite reliable. This led to the breakthrough in [10] where an exact, extremely non linear I-V characteristic was obtained analytically for the interacting resonant level model (IRLM) in the scaling limit, and recovered with remarkable accuracy in td-DMRG simulations on a lattice model. The results can now be used as a benchmark for approximate approaches.

Interesting as it may be, an I-V characteristic does not capture the whole physics of a problem. In fact, the theoretical and experimental activity has concentrated lately on fluctuations, embodied at vanishing temperature by the shot noise. Current fluctuations can be related to the charge of the “elementary” quasiparticles, and their study is akin to a subtle “many-body spectroscopy”.

While the free case has been studied in details [2, 11, 12], progress on the interacting case has been very sparse. Tackling the shot noise certainly increases the level of difficulty. On the analytical side, while the community has slowly accepted the idea that I-V characteristics could

be obtained using the Bethe ansatz (thanks in part to alternate derivations, using all orders perturbation theory [13], or mappings onto an equilibrium system [14]), there is, to our knowledge, only one published exact shot noise calculation [15], which has not yet been confirmed. On the numerical side, extracting the noise from td-DMRG requires looking into the power spectrum of two point correlation functions, a quantity found to be strongly affected by finite size effects.

Nevertheless, it has been realized very recently that the shot noise could indeed be reliably extracted from real time simulations, the finite size effects being controllable partly by analytical arguments, and partly by linear finite size extrapolations [16]. We use this idea to study the noise in the IRLM at the self dual point. Extending and adapting the ideas in [15] we are able to obtain this noise analytically in the scaling limit, while we are also able to carry out the proposal of [16] to determine this noise numerically. These two are in excellent agreement.

The IRLM describes a single fermionic level (d^\dagger) that is coupled to two leads of spinless electrons playing the role of thermodynamical baths (reservoirs of charge and energy). The coupling involves a tunneling term that allows electrons to hop from the leads to the impurity, and an impurity/lead capacitive coupling (Coulombic repulsion U). After the usual procedure of expanding on angular modes, unfolding the leads, and linearizing around the Fermi points, the Hamiltonian is given by:

$$H = H_0 + H_B, \quad H_0 = -i \sum_{a=1,2} \int_{-\infty}^{\infty} dx \psi_a^\dagger \partial_x \psi_a \quad (1)$$

$$H_B = (\gamma_1 \psi_1^\dagger(0) + \gamma_2 \psi_2^\dagger(0)) d + \text{H.c.} \quad (2)$$
$$+ U (:\psi_1^\dagger \psi_1:(0) + :\psi_2^\dagger \psi_2:(0)) (d^\dagger d - \frac{1}{2}) + \epsilon_d d^\dagger d,$$

where the baths are described by two 1D right-moving fields $\psi_a(x)$. The impurity/leads coupling involves the

tunneling amplitudes that we parametrize as:

$$\gamma_1 + i\gamma_2 = \gamma\sqrt{2} e^{i\Gamma/2}. \quad (3)$$

In the following, we consider the (particle-hole symmetric) resonant case with impurity onsite energy $\epsilon_d = 0$.

The IRLM bears a duality symmetry exchanging large and small U 's [19]. For an intermediate value of U (of order unity), it is self-dual, and enjoys an additional, hidden, $SU(2)$ symmetry that mix the two wires, with generators $\vec{J} = \frac{1}{2}\psi_a^\dagger \vec{\sigma}_{ab} \psi_b$ (σ 's are Pauli matrices); as was shown in Ref.10, as a consequence, the out-of-equilibrium self-dual IRLM (sd-IRLM) bears a description in terms of dressed quasiparticles (qp's), that are the many-body modes diagonalizing the scattering on the impurity.

Let us now sketch the main lines of the derivation. As usual in a scattering approach, one starts by identifying two classes of asymptotic states, incoming and outgoing, that correspond to states coming from the far left towards the impurity, and escaping to the far right thereof, respectively. Those states span Hilbert spaces \mathcal{H}_{in} and \mathcal{H}_{out} . The effect of the impurity amounts to a linear map $\mathcal{H}_{\text{in}} \xrightarrow{\mathcal{R}} \mathcal{H}_{\text{out}}$ that encodes the fate of an asymptotic in state prepared in the far past when time-evolved to far future. As soon as there is an interaction, this linear map becomes a complicated many-body object in the electronic basis. Integrability of the IRLM [17] ensures that one can identify a basis for \mathcal{H}_{in} and \mathcal{H}_{out} in terms of pseudo-Fock states built out of a finite number of quasiparticle modes $A_\alpha^{\text{in(out)}}(\theta)$, where θ is a rapidity parametrizing momentum, $p = \frac{m}{2} e^\theta$. Those modes diagonalize the map \mathcal{R} , in the sense that they cross the impurity without qp production, and that this property extends to any many-qp state [18]. The only effect of the impurity is to change the qp index α . Formally, one has:

$$A_\alpha^{\text{in}}(\theta) = R_{\alpha\beta}(\theta) A_\beta^{\text{out}}(\theta) \quad (4)$$

with R a scattering matrix. For the sd-IRLM, such a basis can be obtained via bosonization and a mapping to the anisotropic Kondo model (see [10] for details). The total charge degree of freedom decouples from the problem, and one is left with a single degree of freedom, the charge imbalance between the two wires. The qp's consist of a soliton and an antisoliton A_\pm , and two breathers A_0 and A_1 . Importantly, those qp's fall into representations of the aforementioned $SU(2)$ symmetry: $\{A_\pm, A_1\}$ transform as a spin one, while A_0 is a singlet. The charge imbalance $\hat{Q} = \int dx (\psi_1^\dagger \psi_1 - \psi_2^\dagger \psi_2) = 2 \int dx J^z$ acts diagonally on the modes: $\hat{Q} \cdot A_\alpha(\theta) = q_\alpha A_\alpha(\theta)$, with $q_\pm = \pm 2e$ and $q_{0,1} = 0$. Introducing the operator A_α^\dagger that destroys the qp A_α , the charge \hat{Q} bears a simple representation in terms of the modes: $\hat{Q} = \sum_\alpha \int d\theta q_\alpha A_\alpha(\theta) A_\alpha^\dagger(\theta)$. To complete the description, non-vanishing elements of the R -matrix are $R_{\pm\pm} = \mathcal{Q} - \mathcal{P} \cos^2 \Gamma$, $R_{\pm\mp} = \mathcal{P} \sin^2 \Gamma$, $R_{1\pm} = R_{\pm 1} = \mathcal{P} \frac{\sin(2\Gamma)}{\sqrt{2}}$, $R_{11} = \mathcal{Q} + \mathcal{P} \cos(2\Gamma)$, and R_{00} , with $\mathcal{P}(\theta) = \prod_{k=0,\pm 1} \frac{-i}{e^{\theta - \theta_B + \frac{ik}{3}} + 1}$ and $\mathcal{Q}(\theta) = -ie^{3(\theta - \theta_B)} \mathcal{P}(\theta)$. The lead/impurity coupling results in the appearance of

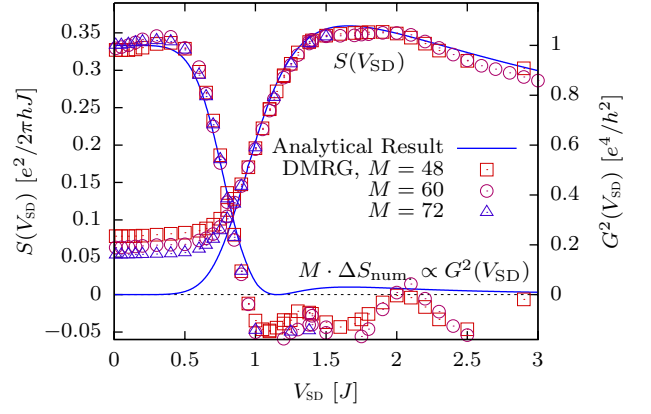


FIG. 1: Finite size error of noise. The blue lines represent the analytical result Eq. (6) with symmetric coupling ($\Gamma = \frac{\pi}{2}$). The numerical data have been obtained for systems with coupling $J' = 0.4J$ and density-density interaction $U = 2.0J$ using td-DMRG. The system size varies from $M = 48$ to $M = 72$ lattice sites. The difference of numerical and analytical data in the low voltage regime is proportional to the squared differential conductance G^2 and scales linearly with the inverse system size $1/M$.

an energy scale $T_B = \frac{m}{2} e^{\theta_B}$ marking the crossover between weak and strong hybridization regimes.

Forcing the sd-IRLM out of equilibrium is achieved by imposing different chemical potentials $\mu_{1(2)} = \pm \frac{V_{\text{SD}}}{2}$ on incoming electronic states in wires 1 and 2, i.e. by coupling the system to $\frac{V_{\text{SD}}}{2} \hat{Q}^{\text{in}} = \frac{V_{\text{SD}}}{2} \int_{-\infty}^0 dx (\psi_1^\dagger \psi_1 - \psi_2^\dagger \psi_2)$. In the qp basis, this operator acts diagonally on the modes A_α^{in} , and the voltage V_{SD} just amounts to a doping of in modes. At zero-temperature and positive voltage, the groundstate is obtained by filling antisoliton states up to a voltage-dependent rapidity $A = \ln(2p_F/m)$ where $p_F \propto V_{\text{SD}}$ is akin to a ‘‘Fermi momentum’’ (because of interactions, the proportionality constant is not one), with distribution function $\rho_-^{V_{\text{SD}}}(\theta)$ that is determined by doing the thermodynamics for the gas of incoming antisolitons.

The current operator counts the charge imbalance between in and out modes, and reads (the factor $\frac{1}{2}$ comes from simple charge counting): $\hat{I} = \frac{1}{2}(\hat{Q}^{\text{in}} - \hat{Q}^{\text{out}})$, that can be rewritten solely in terms of in modes using (4):

$$\hat{I} = \int d\theta A_\alpha^{\text{in}}(\theta) \Pi_{\alpha\beta}(\theta) A_\beta^{\text{in}}(\theta) \quad (5)$$

with $\Pi = \frac{1}{2}(Q - R^*QR)$ and $Q_{\alpha\beta} = q_\alpha \delta_{\alpha\beta}$. Averaging (5) yields $I = \langle \hat{I} \rangle = 2 \sin^2 \Gamma \int_{-\infty}^A d\theta \rho_-^{V_{\text{SD}}}(\theta) \mathcal{T}(\theta)$, with $\mathcal{T} = |\mathcal{P}|^2$. The zero frequency noise in the steady state, $S_0 = \langle \hat{I}^2 \rangle - I^2$, is obtained by averaging the square of (5). The terms $\langle A_\alpha^{\text{in}}(\theta) A_\beta^{\text{in}}(\theta) A_{\alpha'}^{\text{in}}(\theta') A_{\beta'}^{\text{in}}(\theta') \rangle$ that appear have a simple expression at zero temperature [8], and the noise reads: $S_0 = 2 \sin^2 \Gamma \int_0^A d\theta \rho_-^{V_{\text{SD}}}(\theta) [(1 + \sin^2 \Gamma) \mathcal{T}(\theta) - 2 \sin^2 \Gamma (\mathcal{T}(\theta))^2]$. Simple algebraic manipulations using

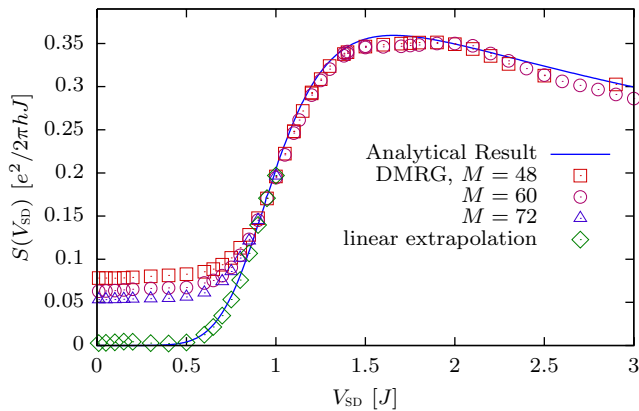


FIG. 2: Linear extrapolation of the numerical shot noise data. The linear scaling of the low voltage finite size error is exploited to perform a linear extrapolation $1/M \rightarrow 0$. We find nice agreement of numerical and analytical results.

the scaling form [10] of the current, $I = V_{\text{SD}} f(\frac{V_{\text{SD}}}{T_{\text{B}}})$, yield:

$$S_0 = \cos^2 \Gamma I + \frac{1}{3} \sin^2 \Gamma (I - G V_{\text{SD}}) \quad (6)$$

with $G = \frac{\partial I}{\partial V_{\text{SD}}}$ the differential conductance. For self-containedness, the scaling function defining the current is: $f(x) = \frac{G_0 \sqrt{\pi}}{2} \bar{f}(\frac{x}{\alpha})$, $\alpha = \frac{4\sqrt{\pi}\Gamma(2/3)}{\Gamma(1/6)}$, $G_0 = G(V_{\text{SD}}=0) = \frac{e^2 \sin^2 \Gamma}{h}$ and $\bar{f}(x) = \sum_{n \geq 0} \frac{(-1)^n (4n)!}{n! \Gamma(3n+3/2)} x^{6n}$ for $x < x^* = \frac{\sqrt{3}}{4^{2/3}}$ while $\bar{f}(x) = \sum_{n > 0} \frac{(-1)^{n+1} \Gamma(1+n/4)}{n! \Gamma(3/2-3n/4)} x^{-3n/2}$ for $x > x^*$.

In the high voltage limit, the Fano factor $S_0/eI \simeq \frac{1+\cos^2 \Gamma}{2} = \frac{\gamma_1^4 + \gamma_2^4}{(\gamma_1^2 + \gamma_2^2)^2}$ is identical to that of free electrons tunneling through a double barrier with tunneling rates proportional to γ_a^2 [20]. Thinking of voltage as a high energy cut-off, this is consistent with the picture of charge carrier being independent electrons [25]. At low voltage, for a symmetric junction $\Gamma = \frac{\pi}{2}$, introducing the backscattered current $I_{\text{BS}} = G_0 V_{\text{SD}} - I$, one obtains $S_0 \simeq 2eI_{\text{BS}}$, i.e. Poissonian noise for charge $2e$ particles, consistent with antisolitons being the charge carriers at low energy.

A completely different approach is based on the numerical simulation of the time evolution of the system. We use the td-DMRG [21] to obtain the time dependent current fluctuations

$$S(t, t') = \langle \Delta \hat{I}(t) \Delta \hat{I}(t') \rangle_{\Psi}, \quad \Delta \hat{I}(t) = \hat{I}(t) - \langle \hat{I}(t) \rangle_{\Psi}, \quad (7)$$

$$\hat{I}(t) = e^{i\hat{H}t} \hat{I} e^{-i\hat{H}t}, \quad \langle \cdot \rangle_{\Psi} = \langle \Psi | \cdot | \Psi \rangle, \quad (8)$$

for a tight-binding lattice version of the IRLM

$$\begin{aligned} \hat{H} &= \hat{H}_0 + \hat{H}_{\text{B}}, \\ \hat{H}_0 &= -J \left\{ \sum_{m=-M_{\text{L}}}^{-2} \hat{c}_{m+1}^{\dagger} \hat{c}_m + \sum_{m=1}^{M_{\text{R}}-1} \hat{c}_{m+1}^{\dagger} \hat{c}_m \right\} + \text{H.c.}, \\ \hat{H}_{\text{B}} &= \sum_{m=\pm 1} \left\{ U(\hat{n}_m - \frac{1}{2})(\hat{n}_d - \frac{1}{2}) - J'(\hat{c}_m^{\dagger} \hat{d} + \text{H.c.}) \right\} + V_{\text{g}} \hat{n}_d, \end{aligned} \quad (9)$$

with the creation, annihilation, and density operators in the leads (\hat{c}_j^{\dagger} , \hat{c}_j , $\hat{n}_j = \hat{c}_j^{\dagger} \hat{c}_j$) and on the level (\hat{d}^{\dagger} , \hat{d} ,

$\hat{n}_d = \hat{d}^{\dagger} \hat{d}$). The total number of sites is given by $M = M_{\text{L}} + M_{\text{R}} + 1$. The time dependent fluctuations then allow for the calculation of the noise power spectrum [24] by means of a Fourier transform $S(\omega) = 4\text{Re} \int_0^{\infty} dt e^{i\omega t} S(t, t')$, where we now restrict ourselves to the low frequency limit $\omega = 0$. Note that the discrete nature of the leads results in a finite bandwidth $4J$ with cosine dispersion. We create an initial state by taking the ground state of $\hat{H} + V_{\text{SD}}(\hat{N}_{\text{L}} - \hat{N}_{\text{R}})/2$, where we added a charge imbalance operator to the system \hat{H} in order to create different fillings in the left and right lead. We now perform a time evolution with respect to \hat{H} and search for a stationary regime close to the impurity, for details see [22].

Within this approach we have to address the following time scales. First, initial oscillations of the current die out on a time scale t_{S} which is typically proportional to the inverse of the resonance width [22, 23]. Second, at transit time $t_{\text{R}} = M/v_{\text{f}}$ the reflections at the boundaries reach the impurity and we have to stop our simulations. Third, after choosing a starting point $t' \gg t_{\text{S}}$ we have to simulate until $t_{\text{max}} < t_{\text{R}}$, where $t_{\text{max}} - t'$ has to be large enough to allow for a faithful calculation of the noise power spectrum. A detailed analysis of the finite size correction in the non-interacting case is provided in [16].

Here, we set $U = 2.0J$, corresponding to the sd-IRLM as discussed in [10], and the coupling to $J' = 0.4J$, while we operate in the resonant tunneling regime $V_{\text{g}} = 0$. The total number of lattice sites varies from $M = 48$ to 72 lattice sites, with $M_{\text{R}} = M_{\text{L}} + 1$. Different other setups have been considered, including the effective enlargement of the system using damped boundary conditions, which will not be presented in this work. For the numerical simulation within the DMRG projection scheme we set an upper bound to the dimension of the Hilbert space for each DMRG block to $N_{\text{cut}} = 4000$ states.

As a first result we compare the numerical data for different system sizes to the analytical result in Fig. 1, where we show zero-frequency shot noise as well as the finite size error of the numerical data, rescaled by the system size. In the low frequency limit, strong finite size effects have to be expected, that get mostly pronounced for small values of the voltage [16]. Since the rescaled finite size error happens to collapse on a single curve in the low voltage regime, the numerical data can be linearly extrapolated to infinite system size in order to obtain results for the thermodynamic limit. Also we verify an analytical estimate for the finite size error $S_{\text{num.}} - S_{\text{analyt.}} \propto G^2/M$ with G the differential conductance that has been given for the free case in [16]. The strong deviations in the high voltage regime from this relation may be traced back to different sources: the approximative td-DMRG scheme introduces a cutoff error that gets especially pronounced for values of the voltage of the order of the bandwidth. Furthermore, to keep the numerical simulation feasible, one has to resort so small systems introducing finite size effects beyond the linear scaling.

Nevertheless, the numerical results shown in Fig. 2, where we obtained data for the low voltage regime using linear extrapolation, show very nice agreement with the

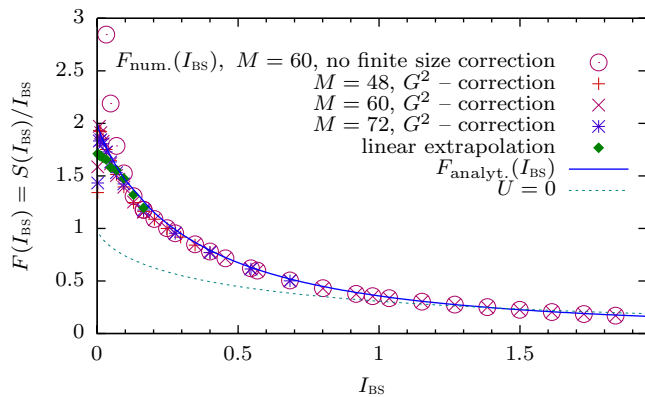


FIG. 3: Back scattering Fano factor as a function of the back scattered current. The numerical data points have been obtained using the numerical shot noise data divided by the analytical back scattered current. The finite size error of the numerical results for shot noise leads to a diverging Fano factor. The situation improves for the linearly extrapolated data, while we find a nice agreement of the analytical result with the G^2 -corrected data. For comparison we show the Fano factor in the non-interacting case.

analytical results given by Eq. (6) with symmetric coupling, $\Gamma = \frac{\pi}{2}$. The back scattering Fano factor $F_{\text{BS}} = S/I_{\text{BS}}$, can also be obtained from the numerical data, Fig. 3, where we use the analytical result for the current [10]. It fits nicely with the analytical result for F_{BS} as long as finite size effects can be neglected. However, the finite size offset at $I_{\text{BS}} \rightarrow 0$ leads to a strongly diverging Fano factor. In contrast, F_{BS} remains finite even for very small values of I_{BS} , when obtained from the linearly extrapolated shot noise data. The deviations from the analytical result at small I_{BS} can be traced back to small absolute errors that

get blown up in the limit $I_{\text{BS}} \rightarrow 0$. The very nice agreement of analytical result and G^2 -corrected data, even in the regime of very small I_{BS} , indicates that increasing the system size and adding more data points to the extrapolation procedure should improve the extrapolated result.

In summary we have provided two different methods, an analytical approach within the framework of the thermodynamic Bethe ansatz, and time dependent DMRG simulations on the lattice to obtain the noise correlations in the IRLM. Both methods show excellent agreement and provide benchmark results for other methods. Most strikingly our results show a strong enhancement of the back scattered Fano factor due to interaction effects.

On the conceptual side, we believe our result further establishes the reliability of the Bethe ansatz approach to transport pioneered in [15]. One of the objections to this approach sometimes raised is that it relies on the theory of excitations over the vacuum, and thus deals with fundamental objects - quasiparticles - which are not simply related to the bare electrons. In the present case, these objects are solitons, of charge $|q_{\pm}| = |2e|$, which are made of combinations of particle hole pairs mixing the two wires. The results in the low energy limit give these quasiparticles their physical reality: they are the objects that tunnel in a Poissonian way at low voltage, and the Fano factor is a direct measure of their charge.

Acknowledgments

The DMRG calculations have been performed on HP XC4000 at Steinbuch Center for Computing (SCC) Karlsruhe under project RT-DMRG. We acknowledge the support by the DFG Center for Functional Nanostructures (CFN), project B2.10.

-
- [1] M. Esposito, U. Harbola, S. Mukamel, *Rev. Mod. Phys.* **81** (2009) 1665.
 - [2] I. Klich, L. Levitov, *Phys. Rev. Lett.* **102** (2009) 100502.
 - [3] R. de Picciotto, M. Heiblum, H. Shtrikman, D. Mahalu, *Phys. Rev. Lett.* **75** (1995) 3340.
 - [4] A. Kumar, L. Saminadayar, D.C. Glattli, Y. Jin, B. Etienne, *Phys. Rev. Lett.* **76** (1996) 2778.
 - [5] B. Reulet, J. Senzier, D.E. Prober, *Phys. Rev. Lett.* **91** (2003) 196601.
 - [6] Y. Bomze, G. Gershon, D. Shovkun, L.S. Levitov, M. Reznikov, *Phys. Rev. Lett.* **95** (2005) 176601.
 - [7] S. Gustavsson, R. Leturcq, B. Simovic, R. Schleser, T. Ihn, P. Studerus, K. Ensslin, *Phys. Rev. Lett.* **96** (2006) 076605.
 - [8] P. Fendley, H. Saleur, *Phys. Rev. B* **54** (1996) 10845.
 - [9] P. Mehta, N. Andrei, *Phys. Rev. Lett.* **100** (2008) 086804.
 - [10] E. Boulat, H. Saleur, P. Schmitteckert, *Phys. Rev. Lett.* **101** (2008) 140601.
 - [11] L.S Levitov, G.B. Lesovik, *JETP lett.* **58** (1993) 230.
 - [12] L. Levitov, H. Lee, G.B. Lesovik, *J. Math. Phys.* **37** (1996) 4845.
 - [13] P. Fendley, F. Lesage, H. Saleur, *J. Stat. Phys.* **79** (1995) 799.
 - [14] V. Bazhanov, S. Lukyanov, A.B. Zamolodchikov, *Nucl. Phys.* **B549** (1999) 529.
 - [15] P. Fendley, A. Ludwig, H. Saleur, *Phys. Rev. Lett.* **75** (1995) 2196.
 - [16] A. Brandschadel, E. Boulat, H. Saleur, P. Schmitteckert, unpublished.
 - [17] V. Filyov, P. Wiegmann, *Phys. Lett.* **76A** (1980) 283.
 - [18] S. Ghoshal, A. Zamolodchikov, *Int. J. Mod. Phys. A* **9** (1994) 3841.
 - [19] A. Schiller, N. Andrei, cond-mat/0710.0249.
 - [20] L. Chen, C. Ting, *Phys. Rev. B* **43** (1990) 4534.
 - [21] P. Schmitteckert, *Phys. Rev. B* **70** (2004) 121302(R).
 - [22] A. Branschädel and P. Schmitteckert, arXiv:1004.4178.
 - [23] N. S. Wingreen, A. P. Jauho, Y. Meir, *Phys. Rev. B* **48** (1993) 8487.
 - [24] Ya. M. Blanter, M. Büttiker, *Phys. Rep.* **336** (2000) 1.
 - [25] Nevertheless, even in the ultraviolet limit the interaction manifests itself as a drastic reduction of the number of hybridized current-carrying states resulting in the suppression of the current $I \sim V_{\text{SD}}^{-1/2}$ – see B. Doyon, *Phys. Rev. Lett.* **99**, 076806 (2007).